Solar Energy 307 (2026) 114340

Contents lists available at ScienceDirect

Solar Energy

journal homepage: www.elsevier.com/locate/solener

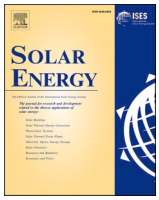

Thermal performance experimental study of a robust funnel solar cooker using an enhanced evaluation method

Celestino Rodrigues Ruivo [a,b,*], Semaan Azize [a], Xabier Apaolaza-Pagoaga [c], Antonio Carrillo-Andrés [c]

[a] Departamento de Engenharia Mecânica, Instituto Superior de Engenharia, Universidade do Algarve, Campus da Penha, 8005-139 Faro, Portugal
[b] ADAI, Department of Mechanical Engineering, Rua Luís Reis Santos, Pólo II, 3030-788 Coimbra, Portugal
[c] Energy Research Group. Department of Mechanical, Thermal and Fluids Engineering, University of Malaga. Calle Arquitecto Francisco Peñalosa, 6, 29071 Malaga, Spain

ARTICLE INFO

Keywords:
Robust funnel cooker
Side by side testing
Mirror degradation
Non-linear performance curve
Enhanced evaluation method

ABSTRACT

The Pucca solar cooker is a domestic funnel-type cooker, constructed of concrete and silvered glass mirrors. Its robust construction allows it to be kept outside permanently, in all weather conditions. However, its reflectors may gradually degrade over time, leading to diminished performance. To assess this issue, six Pucca cookers were tested side by side using a water load of 2 kg in each cooker. Two of the cookers had new mirrors, two had minimally degraded mirrors, and two had badly degraded mirrors. Non-linear efficiency curves were determined by a suitable enhanced evaluation method. Small differences were noted between the efficiency curves of the four cookers with the least degraded reflectors. By contrast, the points of maximum efficiency for the two cookers with badly degraded reflectors amounted to only about 70% of the value seen in the other cookers. The impact of this degradation on performance is illustrated by the figures predicted using the enhanced procedure, where the measured temperature data were fitted to a second-order polynomial with a time-dependent exponential term to derive nonlinear efficiency curves. The best performing cooker is expected to boil 2 kg of water in about three hours when the ambient temperature is 20 °C and the solar irradiance is 700 Wm^{-2}, and in only 1.4 h when the ambient temperature is 30 °C and solar irradiance is 1000 Wm^{-2}. The two cookers with badly degraded mirrors could not boil 2 kg of water at all under either of those conditions. The enhanced method is reliable.

1. Introduction

Despite ongoing efforts to promote solar cooking, most solar cooking devices are not used on a daily basis. Only a small number of individuals, concerned with the use of more ecological cooking solutions, are giving priority to the Sun for cooking, baking and preparing hot drinks in their homes. In a few cases, solar cooking systems are used on a community scale [1,2], or by small businesses, such as bakeries [3,4] and restaurants [5,6]. Data on the importance of solar cooking in the lives of women, and several constraints on the adoption of solar cookers in developing countries, can be found in the literature review of Padonou et al. [7]. Kajumba et al. [8] have determined the amount of energy required to cook several food items selected from Ugandan school menus. Kumar et al. [9] conducted a comparative assessment of eight solar cooking technologies, evaluating their level of technological maturity and their position in the transition from household-scale to institutional-scale cooking. The comparison considered each technology's influence on energy use, economic factors, and environmental performance across its full life cycle.

The most common solar cooking systems operate by using solar energy directly, without any thermal storage process, i.e., the cooking process is possible only during the day time when solar radiation is available. As with any concentrating solar power system, almost every common solar cooking system – panel, box, tube, or parabolic is composed of a reflector and a receiver. The reflectors and receivers are integrated within the same unit.

Panel solar cookers are usually made of a few flat reflectors and the solar radiation concentration ratio of the system is much smaller than systems with parabolic reflectors. The cooking vessel used in most common panel solar cookers must be placed inside a transparent enclosure that acts as a heat trap by creating a greenhouse effect. This is

* Corresponding author at: Departamento de Engenharia Mecânica, Instituto Superior de Engenharia, Universidade do Algarve, Campus da Penha, 8005-139 Faro, Portugal.
E-mail address: cruivo@ualg.pt (C.R. Ruivo).

https://doi.org/10.1016/j.solener.2026.114340
Received 10 October 2025; Received in revised form 25 December 2025; Accepted 13 January 2026
Available online 28 January 2026

Nomenclature

$A_{n,max}$	Maximum area, normal to the sun rays, being collected by the solar cooker (m^2)
$c_{1,0}$	Parameter of Eq. (3) (°C)
$c_{1,1}$	Parameter of Eq. (3) (°C)
$c_{2,0}$	Parameter of Eq. (4) (°C)
$c_{2,1}$	Parameter of Eq. (4) (°C)
$c_{2,2}$	Parameter of Eq. (4) (°C)
I_n	Global normal solar irradiance, i.e., global solar irradiance on the plane normal to beam radiation (Wm^{-2})
$\bar{I}_{n,exp}$	Average value of global normal solar irradiance measured experimentally during a test (Wm^{-2})
$\bar{I}_n$	Average global normal solar irradiance (Wm^{-2})
$\dot{Q}_{s,1000}$	Standardised cooker power at global solar irradiance of 1000 Wm^{-2} (W)
RMSD	Root mean square deviation of fitting temperature curve (°C)
T_a	Ambient temperature (°C)
$\bar{T}_{a,exp}$	Average value of ambient temperature measured experimentally during a test (°C)
T_f	Load temperature (°C)
$T_{f,exp}$	Temperature of the load measured experimentally during a test (°C)
$T_{f,i}$	Initial load temperature value (°C)
$T_{f,f}$	Final load temperature value (°C)
$T_{f,a}$	Load temperature at instant $t = t_a$ (°C)
$T_{f,b}$	Load temperature at instant $t = t_b$ (°C)
t	Time (s)
$t_{a,b}$	Time taken to change the load temperature from a value $T_{f,a}$ to a value $T_{f,b}$ (s)
t_i	Time when load temperature is T_i (s)
t_f	Time when load temperature is T_f (s)
t_1	Parameter of Eq. (3) (s)
t_2	Parameter of Eq. (4) (s)

Greek symbols

χ	Specific temperature difference (m^2 °C W^{-1})
$\Delta T_{f,a}$	Difference between load temperature T_f and ambient temperature T_a (°C)
η	Instantaneous efficiency of a sensible heating load test (−)
Υ	Auxiliary variable defined by Eq. (10) (s °C^{-1})
Θ	Mass of the load in a heating test per unit of maximum aperture area and per heating test time (kg m^{-2} s^{-1})
Ω	Thermal capacitance of the load (J °C^{-1})

essential for successful cooking or baking. The transparent enclosure can be made, for example, of heat resistant plastic or of two suitable clear glass bowls. The time required for cooking or baking using a panel solar cooker depends on the configuration and size of both the reflector and the receiver, the tracking frequency of the reflector, and also obviously on the weather conditions.

Different research teams have employed various approaches to assess the performance of solar cookers. Verma et al. [10] investigated the behaviour of a box solar cooker with a sensible heat storage medium for nocturnal cooking, using a mathematical analytical model. The results provide valuable insights into the optimal charging period for the sensible heat storage medium and help in selecting the appropriate dimensions for the cooking vessel, ensuring efficient operation during both day and night. Goyal and Eswaramoorthy [11] also investigated the performance of a box solar cooker with different arrangements for the sensible heat storage medium, using numerical simulations with COMSOL Multiphysics 6.0 and experimental tests. However, in both of these studies [10,11], performance curves, in terms of efficiency or power, were not presented. In contrast, a recent experimental study on a novel concentrating solar cooker [12], which features a flat heliostat with equatorial tracking and a fixed off-axis paraboloid reflector, clearly presented the efficiency and power performance curves. These curves followed a linear trend, as is commonly adopted by most researchers.

Esen [13] experimentally evaluated a solar cooking system that combined heat pipes with evacuated-tube solar collectors and a well-insulated cooking chamber. Solar energy was captured by a rectangular collector array consisting of six evacuated tubes coupled with six cylindrical parabolic concentrators, providing a total aperture area of 0.96 m2. The absorbed thermal energy was conveyed to the cooking chamber via a heat-transfer fluid. Thermal storage within the chamber was provided by a 7 kg aluminium plate, while a 2.5 kg stainless-steel cooking pot was placed on the plate for cooking and heat retention during evening hours. Six consecutive sensible-heating experiments using 7 kg of water were carried out on a clear day between 08:30 and 20:00 solar time. To demonstrate the system's practical cooking performance and to assess the influence of different heat-transfer fluids, various food items were prepared and their cooking durations measured; however, the load ratios in these cooking tests were considerably lower than those used in the water-heating experiments. The investigated system is more expensive and complex than conventional parabolic and box-type solar cookers; however, it allows indoor cooking, eliminates the risk of glare from concentrated sunlight, and provides significantly higher useful cooking power when the system is preheated.

The time required to heat water from ambient temperature to its boiling point at sea level is one of the parameters used to characterize the thermal performance of box-type solar cookers [14] and parabolic solar cookers [15]. This time is typically estimated using a logarithmic trend. Adopting this trend implies the assumption that the performance curve, expressed in terms of efficiency or cooking power, is linear and that the rate of temperature increase of the load progressively decreases over time. This assumption is consistent with the methodology prescribed in the ASAE S580.1 standard [16] and represents a common approach adopted by most research groups when reporting solar cooker performance.

Collares-Pereira et al. [17] emphasized that a good testing standard is a crucial tool for market development and user acceptance of solar cookers. In this context, they proposed a revision of existing testing procedures with the aim of generating more meaningful and practically useful figures of merit. The proposed approach also assumes that the time required to raise the water temperature from an initial value to a specified target can be estimated using a logarithmic trend, consistent with the methodology commonly adopted in most studies.

To enable a more accurate comparison of different solar cooker designs, it is highly recommended that experiments be conducted simultaneously. Following this approach, Ebersviller and Jetter [18] evaluated three types of solar cookers: a parabolic cooker, a box cooker, and a panel cooker. In their study, the authors measured the amount of water evaporated during the sensible heating tests and found that, for the small panel solar cooker, 6.9% of the initial water mass was lost due to evaporation. This mass loss introduces a non-negligible error in the calculation of cooking power curve, an effect that is not accounted for in standards such as ASAE S580.1 [16].

Tomassetti et al. [19] experimentally analysed the performance of two Kimono solar cooker prototypes, K1 and K2, both featuring adjustable geometries for sun tracking. The two panel-type solar cookers were tested side by side on multiple occasions, under different operating

conditions, both with and without load. A large number of experiments were conducted using 1 kg of water as the load. The shortest heating time for raising the water temperature from 40 to 90 °C was achieved by prototype K2 equipped with receiver R1, requiring 52 min, with a reported aperture area of 0.52 m^2. The authors derived linear performance curves for the standardised cooking power following the procedure proposed by Ruivo et al. [20], which is scientifically consistent and may be regarded as a correction to the method recommended in the ASAE S580.1 standard [16]. It is also worth noting that the cooker opto-thermal ratio values obtained from tests conducted with water and glycerine were derived assuming a linear trend for the efficiency performance curve.

Research perspectives on the most common panel, box, parabolic, and tube solar cookers have recently been presented, drawing on the author's experience as both a practitioner of solar cooking and a researcher involved in reporting the thermal performance of solar cookers [21]. Although scientific studies based on experimental measurements or numerical simulations of load sensible heating processes are widely used to evaluate the thermal performance of solar cookers, it is more critical, and indeed imperative, to address practical aspects from the user's perspective and to complement these studies with real-food cooking tests.

The present work reports on the performance of robust prototype funnel-shaped Pucca solar panel cookers, which are made of concrete and commonly available glass mirrors. These prototypes were designed to be left outside permanently, without risking damage from rain or strong winds. During these tests, the cookers were configured for operation at high sun elevation whenever the average sun elevation angle was above 45°. Water was used as the thermal load, and the cookers were started at the typical time a Portuguese family might begin slow solar cooking, aiming to prepare dishes such as beans or soup for lunch by 1:00p.m. As a result, the tests were conducted during the period before solar noon, rather than during the time period recommended by the ASAE S580.1 standard procedure [16].

Six cookers were tested side by side in a single session in May 2022. Two of the cookers were manufactured in 2022, with new glass mirrors. Another two of the cookers were manufactured more than 10 years before the test session, also with silvered glass mirrors that were new at the time of manufacture. On visual inspection, the mirror panels of all these four cookers appeared to be in good condition, with little or no degradation. The remaining two cookers had also been constructed more than 10 years priori to the test, each flat panel had been fitted, at that time, with several pieces of silvered mirror that had previously been used in other applications. On inspection, the silvered component of most of these pieces, on the back side of the glass, appears to have separated from the glass in many places, and some staining can be seen. Consumers and users of solar cookers would wish to know how long they can expect their investments to last. Testing these six cookers, side-by-side, provide an opportunity to gather important data about the performance at different ages and reflector quality. Further experiments were performed in July 2024, using three solar cookers to check the reproducibility of the results obtained in May 2022. The data analysis follows the procedure described by Ruivo et al. [22]. Specifically, the correlation adopted to fit the measured load temperatures is more accurate than simpler correlations because it captures the non-linear characteristics of the performance curve when expressed in terms of cooking power or efficiency. This approach is therefore consistent with an enhanced evaluation method that enables a more reliable estimation of the time required for sensible heating of water from ambient temperature to its boiling point at sea level. This estimation can differ significantly from that obtained using the simpler procedures commonly adopted to report the performance of solar cooking systems [14,15]. Previous studies have shown that such simplified procedures have questionable applicability to systems whose performance curves deviate substantially from linear behaviour [23,24].

2. Mathematical formulation

The analysis of the performance of common solar cookers is usually accomplished by using a simplified mathematical procedure, which requires only a few items of measured data about the system, like the temperature inside the cooking vessel, the ambient temperature and the solar irradiance, to calculate the performance parameters.

The aperture area of a panel solar cooker, such as the Pucca, is not constant. This is because the reflector was not oriented perfectly towards the sun. So, the value of its maximum collecting area exposed to solar radiation, $A_{n,max}$, is used in the present analysis, and the effect of a smaller effective aperture is interpreted as a reduction in the optical efficiency of the system.

To analyse a sensible heating load test for a load of mass m_f and specific heat $c_{p,f}$, the efficiency depends on the rate of change of the load temperature according to:

$$\eta = \frac{\Omega}{I_n A_{n,max}} \frac{dT_f}{dt} \tag{1}$$

where the thermal capacitance of the load is given by $\Omega = m_f c_{p,f}$. During the test the load temperature T_f rises from the initial value $T_{f,i}$ to a final value $T_{f,f}$, when time t varies from the corresponding initial value t_i to the final value t_f, under a global solar irradiance I_n for the plane perpendicular to the sun rays and ambient temperature T_a. The variation in both variables I_n and T_a during a test should be small, as well as the air velocity, to ensure the applicability of the simplified procedure adopted, namely also when calculating the specific temperature difference χ defined, by:

$$\chi = \frac{T_f - T_a}{I_n} \tag{2}$$

The efficiency curve of the cooker associated with the transient heating process of the load can be obtained by calculating first, for several instants, the values of the efficiency η and the specific temperature difference χ, or by fitting an adequate polynomial function that represents analytically, with enough accuracy, the way the temperature of the load varies during the test. A procedure analogous to the ones originally developed for reporting the performance of solar collectors under steady-state conditions [25] has been used in several published studies [26–28]. When adopting the Hottel-Whillier-Bliss (HWB) formulation [25], a linear curve of η versus χ is obtained. This simplified formulation was used by Ruivo et al. [20] to point out the need to correct the standard ASAE S580.1 procedure [16]. It also supports the procedure for deriving the opto-thermal ratio of a cooker [26,27]. When deriving the linear efficiency curve, it is assumed that the measured load temperature $T_{f,exp}$ varies according to a first order polynomial, being the argument of an exponential function of time, i.e., by the following expression [22]:

$$T_{f,exp} = c_{1,1} \exp\left(-\frac{t}{t_1}\right) + c_{1,0} \tag{3}$$

which is equivalent to

$$t = -t_1 \ln\left(\frac{T_{f,exp} - c_{1,0}}{c_{1,1}}\right) \tag{4}$$

The values of the constants $c_{1,1}$, $c_{1,0}$ and t_1 are determined, for example, using the Excel Solver tool, with the objective of minimizing the difference between the values predicted by Eq. (3) and the experimentally measured data. The constant $c_{1,0}$ can be interpreted as the theoretical maximum temperature that the load can reach under the experimental conditions of the test, assuming no phase change occurs. The time-dependent trend described by Eq. (3) is consistent with the adopted approach by most research groups, including Collares-Pereira et al. [17], Mullick et al. [14], and Mullick and Kandpal [15]

As example, this kind of approach was also recently adopted in the

study performed by Alonso et al. [12] by taking into account the simplified formulation used by Ruivo et al. [20]. In the present work, the performance results of the solar cooker obtained by the fitting of Eq. (3) are not presented because, as demonstrated in the previous work of Ruivo et al. [22], these performance indicators can be inappropriate for some solar cooker designs. Thus, in the present work, the performance results are derived solely from the best fitting, which was also used in the previous work of Ruivo et al. [22], and is expressed by:

$$T_{f,exp} = c_{2,2}\left(\exp\left(-\frac{t}{t_2}\right)\right)^2 + c_{2,1}\exp\left(-\frac{t}{t_2}\right) + c_{2,0} \quad (5)$$

The constants $c_{2,2}$, $c_{2,1}$, $c_{2,0}$ and t_2 were determined with the EXCEL Solver software considering as goal the minimisation of the differences between the temperature values predicted by Eq. (5) and the experimental measured temperature, i.e., minimisation of the root mean square deviation. These constants are valid for the conditions imposed during the experiment by the values of the solar irradiance, the ambient temperature and the air velocity. When there are small variations in these variables during the experiment, the average values of the solar irradiance $\bar{I}_{n,exp}$ and ambient temperature $\overline{T}_{a,exp}$ are adopted as a simplifying assumption. By following Ruivo et al. [22], the efficiency, at any instant, for the conditions of the experiment, can be expressed as:

$$\eta = \frac{-\Omega}{A_{n,max}\bar{I}_{n,exp}}\left(\frac{2c_{2,2}}{t_2}\left(\exp\left(-\frac{t}{t_2}\right)\right)^2 + \frac{c_{2,1}}{t_2}\exp\left(-\frac{t}{t_2}\right)\right) \quad (6)$$

Previous experiments demonstrated that the trend of the efficiency curve expressed by Eq. (6) corresponds to the trend of the efficiency curve depicted in Fig. 1a. In this graphical representation, the points B and C represent, respectively, the instants when the load achieves the boiling point of water, and when the system achieves the point of maximum efficiency. It is important to point out that, in this definition of the system, only the thermal capacitance of the load is used in calculating the power used in the calculation of efficiency by Eq. (1). The thermal capacitances of other components of the cooking vessel obviously impact on the transient behaviour of the system, but their values are not considered in the calculation of the efficiency. The dashed portions of the lines, in the load temperature and in the efficiency curves, shown in Fig. 1a represent an extrapolation of the trend that could exist if phase change phenomena inside the system were not occurring, such as when glycerine, or another intermediate heat transfer fluid, is used instead of water.

Knowing the values of constants $c_{2,2}$, $c_{2,1}$, $c_{2,0}$ and t_2, it is possible to calculate, for each instant, the temperature of the load using Eq. (5), the efficiency using Eq. (6), the specific temperature difference using Eq. (2), and then plot the efficiency curve as a function of the specific temperature difference, as shown in Fig. 1b. According to Ruivo et al. [22], this can be written as:

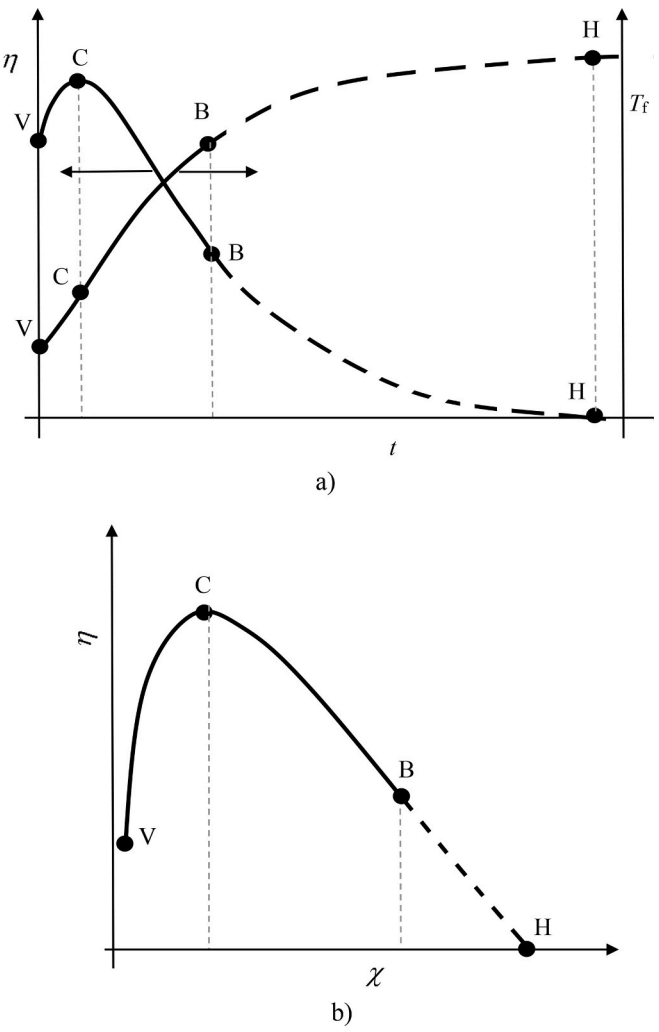

Fig. 1. Schematic representation of: a) time evolution of the load temperature and efficiency and b) non-linear efficiency curve.

$$\eta = \frac{-\Omega\left(c_{2,1}\sqrt{c_{2,1}^2 - 4c_{2,2}\left(c_{2,0} - \chi\bar{I}_{n,exp} - \overline{T}_{a,exp}\right)} + c_{2,1}^2 - 4c_{2,2}\left(c_{2,0} - \chi\bar{I}_{n,exp} - \overline{T}_{a,exp}\right)\right)}{2c_{2,2}t_2A_{n,max}\bar{I}_{n,exp}} \quad (7)$$

The point C represents the instant where the system exhibits its maximum efficiency, i.e., it marks the point in the curve where the efficiency stops increasing and begins to decrease. The shape of the initial part is, at first sight, difficult to understand. One explanation is that the other components of the cooking system also store part of the solar radiation with a temperature variation rate that differs from the temperature variation rate of the load. Part of the deviation from the linear trend, for the whole period of the test, can also be attributed partially to changes of the optical efficiency associated with the variations in solar altitude angle for the case where the reflector is only adjusted azimuthally.

In solar cooking systems with an efficiency curve deviating significantly from the most common linear trend, point B is usually achieved after point C, as shown in Fig. 1b. As mentioned before, the dashed line shown after point B is an extrapolation of the curve obtained with data from a test using water as a load, with point H interpreted as a theoretical load stagnation temperature point where the efficiency is zero. Point V corresponds to the point at $t = 0$ s, i.e., when the load heating process begins.

It can be demonstrated from Eq. (6), that the maximum efficiency value is reached when:

$$\exp\left(-\frac{t}{t_2}\right)=\frac{-c_{2,1}}{4c_{2,2}} \tag{8}$$

and the value is given by:

$$\eta=\frac{\Upsilon}{8}\frac{c_{2,1}^2}{c_{2,2}t_2} \tag{9}$$

where the auxiliary variable Υ is a parameter expressed by:

$$\Upsilon=\frac{\Omega}{A_{n,max}\bar{I}_{n,exp}} \tag{10}$$

Manipulating Eqs. (5) and (6), and taking into account the definition of specific temperature difference expressed by Eq. (2), the efficiency and the specific temperature difference of points V, C and H can be estimated as follows:

$$\chi_V=\frac{c_{2,2}+c_{2,1}+c_{2,0}-\overline{T}_{a,exp}}{\bar{I}_{n,exp}} \tag{11}$$

$$\eta_V=-\Upsilon\frac{(2c_{2,2}+c_{2,1})}{t_2} \tag{12}$$

$$\chi_C=\frac{c_{2,0}-\frac{3c_{2,1}^2}{16c_{2,2}}-\overline{T}_{a,exp}}{\bar{I}_{n,exp}} \tag{13}$$

$$\eta_C=\Upsilon\frac{c_{2,1}^2}{8t_2c_{2,2}} \tag{14}$$

$$\chi_H=\frac{c_{2,0}-\overline{T}_{a,exp}}{\bar{I}_{n,exp}} \tag{15}$$

$$\eta_H=0 \tag{16}$$

The coordinate χ_V of point V is equal to zero only when the initial temperature of the load is strictly equal to T_a. The coordinate χ_H of point H can be recognised as the cooker opto-thermal ratio established by Lahkar et al. [26] that has usually been derived from the linear efficiency curve over the whole range of χ. Thus, the accuracy of the procedure based on the cooker opto-thermal ratio to estimate the duration of change of the load temperature, following, for example, Eq. (27) in Ruivo et al. [24], and appearing also in several other published studies, is only applicable to cookers exhibiting a linear efficiency curve, i.e., when the temperature of the load fits the polynomial function expressed in Eq. (3). So, if the efficiency curve departs significantly from the linear, the use of the opto-thermal ratio to determine, in a simplified way, for example, the time needed for the load to change its temperature from one value to another, may be questionable.

Even though the constants $c_{2,2}$, $c_{2,1}$, $c_{2,0}$ and t_2 were derived from experimental data produced under certain conditions of solar irradiance $\bar{I}_{n,exp}$, ambient temperature $\overline{T}_{a,exp}$ and air velocity of each test, the derived efficiency curve can be applied to other particular values of solar irradiance I_n and ambient temperature T_a. At a particular instant, for the conditions of the experiment, the particular corresponding value of the specific temperature difference is given by:

$$\chi=\frac{T_{f,exp}-\overline{T}_{a,exp}}{\bar{I}_{n,exp}}=\frac{c_{2,2}\left(\exp\left(-\frac{t}{t_2}\right)\right)^2+c_{2,1}\exp\left(-\frac{t}{t_2}\right)+c_{2,0}-\overline{T}_{a,exp}}{\bar{I}_{n,exp}} \tag{17}$$

Taking into account both Eqs. (2) and (17) and the condition $\chi=\chi_{exp}$, the time evolution of load temperature, for any other case with particular values of solar irradiance I_n and the ambient temperature T_a, can be predicted by:

$$T_f=\left(c_{2,2}\left(\exp\left(-\frac{t}{t_2}\right)\right)^2+c_{2,1}\exp\left(-\frac{t}{t_2}\right)+c_{2,0}-\overline{T}_{a,exp}\right)\frac{I_n}{\bar{I}_{n,exp}}+T_a \tag{18}$$

According to Ruivo et al. [22], it is possible to derive, from Eq. (54), the following relationship:

$$\exp\left(-\frac{t}{t_2}\right)=\frac{-c_{2,1}-\sqrt{c_{2,1}^2-4c_{2,2}(c_{2,0}-T_{f,exp})}}{2c_{2,2}} \tag{19}$$

This can be used to derive the inverse function of the function expressed by Eq. (54) as:

$$t=-t_2\ln\left(\frac{-c_{2,1}-\sqrt{c_{2,1}^2-4c_{2,2}(c_{2,0}-T_{f,exp})}}{2c_{2,2}}\right) \tag{20}$$

For any other cases with particular values of solar irradiance I_n and the ambient temperature T_a, the inverse function of the function expressed by Eq. (18) becomes:

$$t=-t_2\ln\left(\frac{-c_{2,1}-\sqrt{c_{2,1}^2-4c_{2,2}\left(c_{2,0}-\left(\overline{T}_{a,exp}+(T_f-T_a)\frac{\bar{I}_{n,exp}}{I_n}\right)\right)}}{2c_{2,2}}\right) \tag{21}$$

Thus, due to the limitations of applicability of the simplified formulation based on the opto-thermal ratio for determining the time taken to change the load temperature from a value $T_{f,a}$ to a value $T_{f,b}$, it is recommended that it should be estimated from the following derived expression:

$$t_{a,b}=-t_2\ln\left(\frac{c_{2,1}+\sqrt{c_{2,1}^2-4c_{2,2}\left(c_{2,0}-\left(\overline{T}_{a,exp}+(T_{f,b}-T_a)\frac{\bar{I}_{n,exp}}{I_n}\right)\right)}}{c_{2,1}+\sqrt{c_{2,1}^2-4c_{2,2}\left(c_{2,0}-\left(\overline{T}_{a,exp}+(T_{f,a}-T_a)\frac{\bar{I}_{n,exp}}{I_n}\right)\right)}}\right) \tag{22}$$

For tests using a cooking vessel loaded with water, the constants $c_{2,2}$, $c_{2,1}$, $c_{2,0}$ and t_2 are derived by using experimental measured data from the initial instant to a final instant where the water temperature reaches a value close to its boiling temperature minus 5 °C. As mentioned before, the point B represents a point associated with the boiling process of water with temperature $T_{f,B}$, which depends on the system pressure. The efficiency of the process at point B, for a case with particular values of solar irradiance I_n and the ambient temperature T_a, can be predicted by first determining the specific difference temperature:

$$\chi_B=(T_{f,B}-T_a)/I_n \tag{23}$$

and then using Eq. (7) to calculate η_B by considering $\chi=\chi_B$.

The standardised cooking power for a solar irradiance of $I_n=1000$ Wm^{-2} at a particular instant t can be estimated by:

$$\dot{Q}_{s,1000}=\eta I_n A_{n,max} \tag{24}$$

where the efficiency η is determined by Eq. (6). The corresponding particular value of the difference between load and ambient temperature, $\Delta T_{f,a}=T_f-T_a$, at the same instant t can be estimated by:

$$\Delta T_{f,a}=\left(c_{2,2}\left(\exp\left(-\frac{t}{t_2}\right)\right)^2+c_{2,1}\exp\left(-\frac{t}{t_2}\right)+c_{2,0}-T_{a,exp}\right)\frac{I_n}{\bar{I}_{n,exp}} \tag{25}$$

and the corresponding specific temperature difference χ by its definition expressed by Eq. (2).

The average efficiency during the load sensible heating period, from temperature $T_{f,a}$ at time t_a to $T_{f,b}$ at time t_b, can be evaluated as follows:

$$\overline{\eta}_{a,b} = \frac{\Omega\left(T_{f,b} - T_{f,a}\right)}{A_{n,max}\overline{I}_{n,exp}t_{a,b}} \tag{26}$$

It is convenient to define a ratio Θ as the mass of the load in a heating test per unit of maximum aperture area and per heating test time, i.e., a specific cooking rate:

$$\Theta = \frac{m_f}{A_{n,max}t_{a,b}} \tag{27}$$

By using Eq. (25), this ratio can be expressed as follows:

$$\Theta = \overline{\eta}_{a,b}\frac{\overline{I}_{n,exp}}{c_{p,f}\left(T_{f,b} - T_{f,a}\right)} \tag{28}$$

When expressed in kg $m^{-2}h^{-1}$, the specific cooking rate becomes a practical and convenient parameter for comparing experimental results from different cooker designs reported by various researchers, particularly when not all essential test data are provided in the original reports. The specific cooking rate represents the mass of load that can be heated from $T_{f,a}$ to $T_{f,b}$ in a one-hour test if the cooker design had an aperture area of 1 m^2.

The entire formulation procedure presented in this section is supported by measured experimental data and can be applied to report the performance of common types of solar cookers, including panel, parabolic, and box cookers. The results are strictly valid for the specific cooker configuration tested and the conditions of the experiment. The derived efficiency curve can be used to predict the performance of the tested solar cooker under different solar irradiance and ambient temperature values, provided the sun elevation follows a similar evolution to that observed during the experiments.

It is important to highlight that: i) the wind speed was measured near the cookers using a sensor that does not capture the wind direction, and ii) the effect of the measured wind speed on the performance of the solar cookers is not incorporated into the mathematical model. Therefore, within the scope of this study, the impact of varying wind speed intensity and direction is assumed to have a negligible effect on the overall thermal resistance between the cooking pot and the ambient air. This assumption would likely be questionable if the cooking vessel, containing the load, is directly exposed to the wind. This is not the case for the Pucca cooker, as it uses a glass enclosure, nor is it the case for a box-type cooker. In this study, the measured ambient temperature is assumed to represent the average temperature of the surrounding surfaces that influence thermal losses due to radiative heat transfer. Such an assumption is commonly adopted by most research teams reporting the performance of solar cookers based on experimental data. Various approaches based on analytical and numerical mathematical models have been used to simulate the thermal behaviour of box cookers [10,11]. However, the evaluation of thermal losses through the glass cover is often simplified by applying Newton's law of cooling with a fixed value for the external heat transfer coefficient. This method does not account for the effects of wind speed and direction on the performance of the solar cooker. Accurately simulating the interaction between wind and the cooker would require a sophisticated Computational Fluid Dynamics model (CFD), which is a complex and computationally demanding task. Therefore, procedures based on experimentally measured data can be considered both useful and a reasonable compromise.

Current procedures for reporting the performance of solar cookers are primarily based on the sensible heating of a load. Therefore, developing a standardized procedure that also evaluates performance during the water boiling process is an important topic that warrants further investigation through experimental testing.

In the thermal procedures presented for box solar cookers [14] and parabolic solar cookers [15], the mathematical expression used to estimate the sensible heating of water from ambient temperature to the boiling point at sea level implicitly assumes that the water temperature during the sensible heating tests follows an exponential trend, as expressed by Eq. (3). This assumption is equivalent to considering linear efficiency and power performance curves, which may not be valid for certain solar cooker designs [22]. In contrast, the use of Eq. (22) to estimate sensible heating time has a broader range of applicability, as it does not rely on the assumption of linear performance curves. Nevertheless, despite certain limitations, this aspect represents an important and innovative contribution of the approach here adopted for reporting the performance of the Pucca solar cooker.

3. Experimental set-up and testing procedure

3.1. Brief description of the Pucca solar cooker design

The Pucca solar cooker design investigated in the present study was invented in 2009 by the author, Celestino Ruivo, as a result of his experience in constructing and using low-cost, foldable panel solar cookers for practical cooking applications and solar cooking workshops.

Fig. 2 shows a Pucca solar cooker manufactured in 2010, fitted with new glass mirrors. This cooker design is composed of three main heavy pieces. The base, weighing 30.2 kg, has a vertical pin that serves as a rotation axis, enabling azimuthal rotation of the other two parts of cooker. The second part is a concrete block weighing 28.7 kg, with a vertical cylindrical hole for the vertical pin, and a horizontal mirror, on which the cooking vessel is located. The third, and main part, is placed on top of the second part. This upper part, also made of concrete weighing 89.3 kg, is funnel-shaped, and covered with glass mirrors.

The reflector shape of the Pucca solar cooker is closely similar to that of the lightweight funnel design previously tested under both low sun elevation conditions [29,30] and high sun elevation conditions [31]. The flat glass mirror panels reflect the sun's rays onto the cooking vessel. The cooking vessel sits on a horizontal glass mirror measuring 220 mm $\times$ 200 mm, that is fixed to the concrete block. The cooking zone of the funnel cooker tested in a previous study at high sun elevation [31] differs from that of the Pucca cooker design due to differences in the cooking vessel supports.

The cooker depicted in Fig. 2 is being used on the roof terrace of a family home located in Faro, Portugal (latitude: 37.0°N, longitude: 7.9°W). The photos show front and side views of the cooker, configured to operate at high sun elevations. In this configuration, good optical performance is expected when the solar altitude angle is close to 53°. However, the system can be reconfigured for operation under low solar positions. In this low-sun configuration, the best optical performance is expected when the solar altitude angle is close to 37°. Switching between low and high sun configurations is a simple operation that can be performed by the user by tilting the funnel component.

In the set shown in Fig. 2, the base is directly positioned over the floor. This cooking device is very robust. This means that i) unlike most lightweight panel cookers, it can be used on very windy days because the reflector and the cooking vessel both remain stable and maintain their positions during very high winds and ii) it can be kept permanently outside in all weather conditions, which is another important aspect well appreciated by the frequent user, cooking on a daily basis.

Solar tracking of the system azimuthally by rotating both funnel and block parts is easy. The funnel part is usually tilted in one of two positions, one when sun elevation is low and other when sun elevation is high. At Faro's latitude, the maximum solar elevation angles at the winter and summer solstices are approximately 26.5° and 73°, respectively.

The maximum possible collection area for incoming solar radiation is estimated to be 0.52 m^2.

The cooking vessel usually used is a black enamelled steel pot of 3 L

a) b)

Fig. 2. Pucca solar cooker position for high sun elevation operation: a) front view and b) side view.

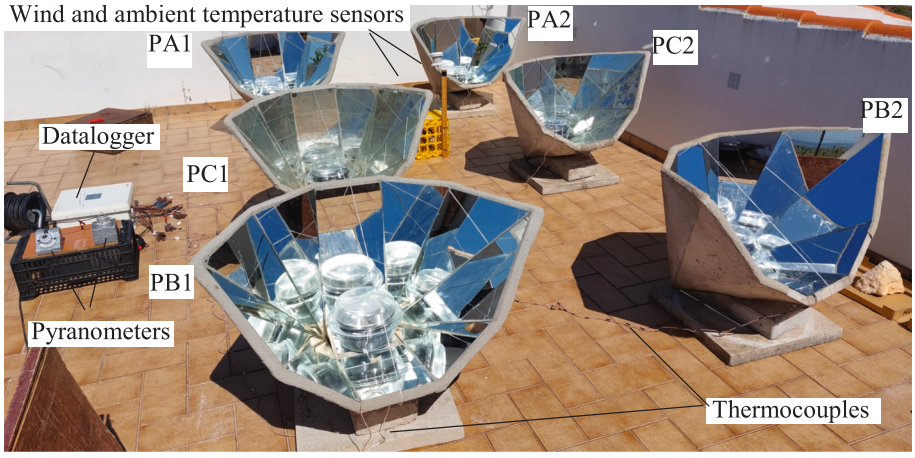

a)

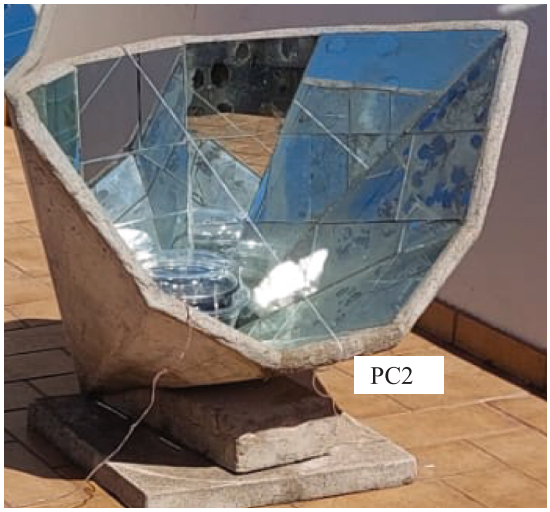

b)

Fig. 3. Experimental set-up: a) set of six Pucca solar cookers being tested side by side and b) Pucca solar cooker PC2 with degraded mirrors.

capacity, covered with a glass lid or a metal lid, and surrounded by a massive transparent glass enclosure. The glass enclosure is used to promote the greenhouse effect around the pot. It is made of two particularly thick glass bowls. The cooking pot inside the glass enclosure acts as receiver, but, if a glass lid is used on the top of the pot, part of the solar radiation is also absorbed directly by the food being cooked.

Appendix A presents supplementary details on the construction, estimated costs, and practical use of this solar cooker design.

3.2. Experimental set-up

Fig. 3a shows the experimental set-up, on the roof of a family house, used to test six Pucca cookers side by side. These cookers, PA1, PA2, PB1, PB2, PC1 and PC2 were tested, with loads, on 27th May 2022. The two cookers with new glass mirrors, cookers PA1 and PA2, were located in the back row, the two cookers with glass mirrors showing a minor amount of mirror degradation, cookers PB1 and PB2, were located in the front row, and the other two cookers, PC1 and PC2, made of glass mirrors with a high level of mirror degradation, were located in the middle row. Fig. 3b shows a close-up view of the view of the degraded layer of silver in almost all glass mirror components of cooker PC2.

Each pot has a mass of 540 g and is made of enamelled steel with shiny black surface, a wall thickness of 0.9 mm, and is 100 mm high and a 200 mm external diameter. The lid of the pot has a 207 mm diameter, weights 366 g, and is made of 3.9 mm thick clear glass with a metal ring at the circumference. The two pieces of the transparent glass enclosure are made of 5 mm clear glass. The total mass of each complete unloaded cooking vessel was approximately equal to 3140 g.

Five type-T thermocouples, with an operational range of −75 to 250 °C and tolerance of ± 1.0 °C, were installed inside each pot, to measure the temperature of the water in five different positions. The average values of the temperature measured by this set of sensors during short time intervals were assumed to represent accurately the dynamic time variation of the average temperature of the water (T_f), which is used in the calculations of parameters η and χ.

The ambient air temperature was measured by a thermistor sensor *S*-TMB-M002 (operation range: −40 to 75 °C, accuracy: ±0.2 °C from 0 to 50 °C) and logged every minute by the Onset weather station, located near the solar cookers. The ambient temperature (T_a) used in the calculations is estimated to be the average of the values measured by this sensor of ambient air temperature during the whole experiment. The wind speed values were measured by a cup anemometer *S*-WSB-M003 (operational range: 0 to 76 m s^{-1}, accuracy: 1.1 m s^{-1} ± 4% of reading, whichever is greater, resolution: 0.5 m s^{-1}) and logged every minute by the same Onset weather station. The cup anemometer *S*-WSB-M003 is placed at a height of 50 cm and close to the ambient temperature sensor. It is not visible in photo shown in Fig. 3a because it is behind cooker PC1.

The values of the wind speed were not used to estimate η and χ. They were measured just to check if, for most of the experiment, the wind velocity was relatively low, a condition that must be satisfied to consider the experiment as a low wind velocity experiment.

The global solar irradiance, I_n, in the plane perpendicular to the sun rays, and used in the calculations of parameters η and χ, was not directly measured by a single pyranometer, perfectly tracking the sun. Instead, it was found convenient to estimate the global solar irradiance, I_n, on that plane, by using the Liu Jordan isotropic sky model [25]. As in previous studies [29–31], two Hukseflux LP02 pyranometers were used to measure global solar irradiance on different planes. The operating range of both pyranometers is 0 to 2000 W/m^2, and their calibration uncertainty is less than 1.8%.

One pyranometer was installed horizontally on the upper part of a small cubic wooden block, and the other pyranometer was installed on the tilted surface of another small wooden block, making an angle of 50° with the horizontal plane. The tilted pyranometer was azimuthally adjusted every 20 min. The experiments were conducted under conditions of a clear sky day.

Every 15 s the values measured by the temperature and solar irradiance sensors were logged by a Campbell Scientific CR1000 data logger. Then, the mean value of each measured variable was calculated for every minute.

The data measured in each cooker when load temperature is higher than 95 °C were not used in the calculations to derive the cooker performance curves.

During the experiment, the solar cookers were adjusted for high sun operation and the tilted pyranometer was tracked azimuthally approximately every 20 min.

Funnel cookers, as used in the present study, are composed of multiple flat mirrors that can been considered to be panel solar cookers intended for cooking a relatively high mass of food for between 2 h and 3 h. For this reason, in the present study, each cooker was tested with 2 kg of water, i.e., with a load ratio of 4.0 kg m^{-2} and not with a relatively high load ratio of 7.0 kg m^{-2} as recommended by ASAE S580.1 [16].

4. Experimental tests performed and discussion of the results

4.1. Single side by side test of six solar cookers

The test conducted with the six cookers depicted in Fig. 3a started at around 10:10, local time, and ended at 12:55, on 27th May 2022. This testing period is usually used to solar cook lunch in this household, i.e., before solar noon. On the day of this test, solar noon corresponded to 13:30, local time.

The data measured when the load temperature ranged from 95 °C to 100 °C were not used in the calculations to derive the efficiency curve of the cooker. Fig. 4a shows the plots of the solar irradiance, the ambient temperature and the load temperature observed during the experiment. At the end of experiment, the water in the four fast cookers (PA1, PA2, PB1 and PB2) achieved its boiling point. In one of the slow cookers (PC2), testing stopped when the temperature of the water was not greater than 95 °C, as was planned, but its final value was close to 95 °C. Thus, the time required for the water temperature to reach 95 °C, or close to 95 °C, differed from one cooker to another. Fig. 4b shows how the sun elevation varied during the experiment. The measured data used in the calculations for the faster cooker corresponds to the period of sun elevation from 45° to 61.9° and for the two slow cookers corresponds to sun elevations between 45° and 72.6°. Fig. 4b shows also the air velocity measured by a resolution anemometer of 0.5 m s^{-1}. Table 1 summarizes the data associated with each tested cooker: the initial and final sun elevation, average values for air velocity, air temperature and solar irradiance, parameter Υ and the constants of the load temperature evolution. The GRG Nonlinear engine of Solver tool of MS EXCEL was used to determine the constants $c_{2,0}$, $c_{2,1}$, $c_{2,2}$ and t_2 for each cooker by using the respective experimental data when load temperature ranged from initial value to 95 °C, the value of boiling point of water at the location minus 5 °C, and adopting the fitting curve for the load temperature of each cooker, in the form of Eq. (5). In the same table, the root mean square deviation is listed. The values of the auxiliary variable Υ, parameter, defined by Eq. (10), would be equal for all cookers if the time interval used in the fitting procedure of the load temperature of each cooker, were the same. The small observed differences led to the changes

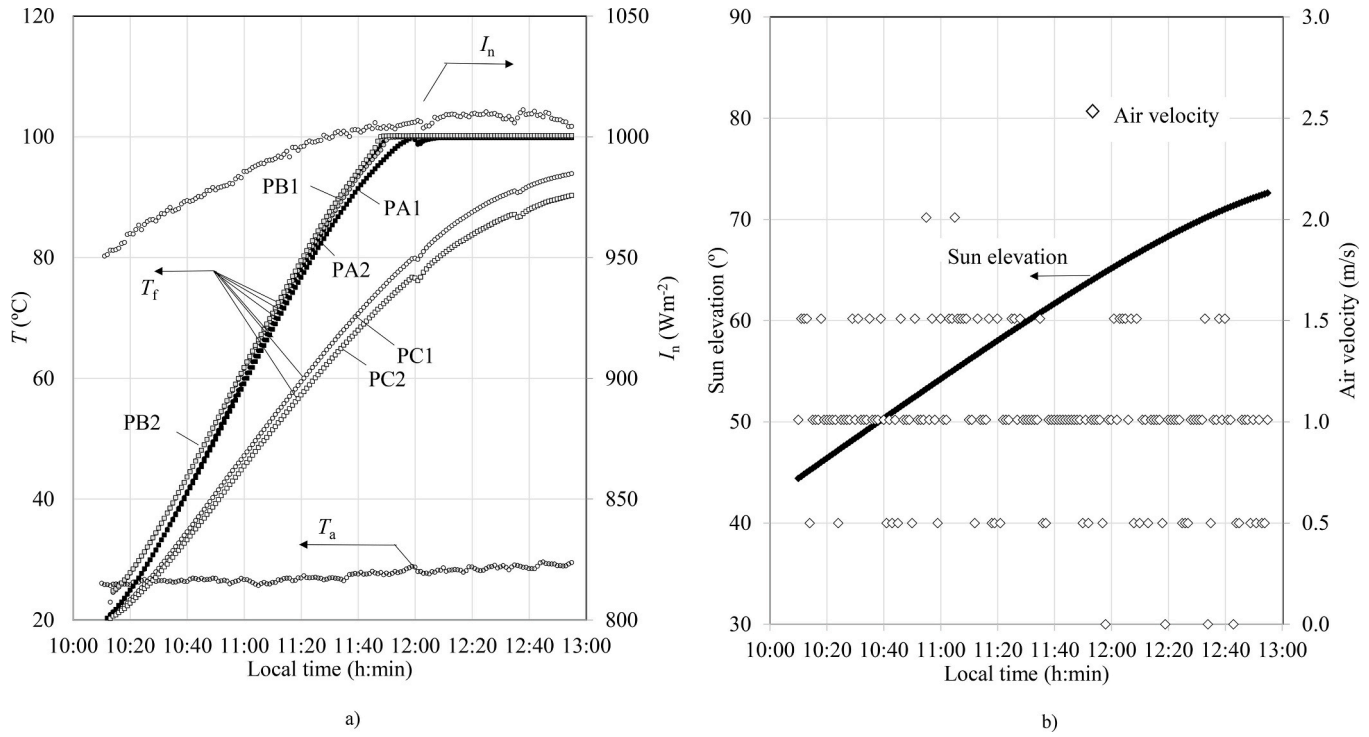

Fig. 4. Experimental data from testing Pucca cookers loaded with 2 kg of water on 27th May 2022: a) solar irradiance, load temperature and ambient temperature and b) air velocity and sun elevation.

Table 1
Experimental data associated with each tested cooker on 27th May 2022.

Cooker	PA1	PA2	PB1	PB2	PC1	PC2
Initial sun elevation (°)	45.0	45.0	45.0	45.0	45.0	45.0
Final sun elevation (°)	62.0	62.8	62.0	61.9	72.6	72.6
Average air velocity (m s^{-1})	1.1	1.1	1.1	1.1	1.0	1.0
Average air temperature (°C)	26.6	26.6	26.6	26.6	27.4	27.4
Average solar irradiance (Wm^{-2})	982.1	983.0	982.1	981.9	993.4	993.4
Parameter Υ (s °C^{-1})	16.37	16.35	16.37	16.37	16.18	16.18
$c_{2,0}$(°C)	154.6	145.1	150.0	152.5	108.6	103.5
$c_{2,1}$(°C)	−233.6	−217.7	−218.7	−226.8	−160.5	−154.0
$c_{2,2}$(°C)	99.8	93.6	92.6	98.5	73.0	71.5
t_2(s)	4327.0	4099.7	4280.2	4246.7	3963.5	3891.0
RMSD(°C)	0.077	0.187	0.062	0.134	0.507	0.407

in the average values of $I_{n,exp}$.

4.2. *Performance data derived from the single side by side test of six solar cookers*

By knowing the values of the constants in Eq. (5) derived from experiment conducted on 27th May 2022 and listed in Table 1, Eq. (6) was used to determine the performance curves for each cooker. Fig. 5a and 5b show efficiency curves and Fig. 5c shows the standardised cooking power $\dot{Q}_{s,1000}$ curves. The coordinates of points V, C and H, particular points of the efficiency curve, are listed in Table 2. The values of χ_V are close to zero. They are not exactly zero, mainly because the initial temperature of the load does not exactly match the average ambient air temperature. Thus, the listed values of η_V are close to the efficiency when $\chi = 0$ °C m^2 W^{-1}. It is important to highlight that in this formulation, η_V does not correspond to the physical concept of optical efficiency, as is the case when the efficiency curve is linear. That is, when the load temperature depends on time according to the fitting expressed by Eq. (3).

In the authors' opinion, the non-linear trend of the efficiency curve may be attributed to: i) a significant difference between the time evolutions of the temperatures of the massive glass enclosure and the load, and possibly a slight difference between the time evolutions of the temperatures of the non-massive pot and the load; and ii) changes in the real aperture area and optical efficiency of each cooker during the testing period.

In the authors' opinion, if the mass of the glass enclosure were negligible and each cooker were perfectly oriented in both axes with precise sun tracking, the efficiency curve would be expected to follow a trend closer to linear. Specific tests should be planned to investigate this important behaviour of the efficiency curve, though this task is outside the scope of the present study.

From Fig. 5, it can be concluded that cooker PC1 performs a little better than cooker PC2, but the performances of both cookers PC1 and PC2 are poor when compared with the other four cookers PA1, PA2, PB1 and PB2. The differences in the efficiency values of these four cookers at point, η_C, are small, but the average efficiency value of these four cookers is 43% greater than the efficiency η_C of the other two cookers. Even though the tests were done with water as the load, each curve in Fig. 6 also shows, using a dashed line, that at load temperatures greater than the boiling point of water, the relationship is almost linear. As expected, the solar cookers PC1 and PC2 perform poorly due to visible

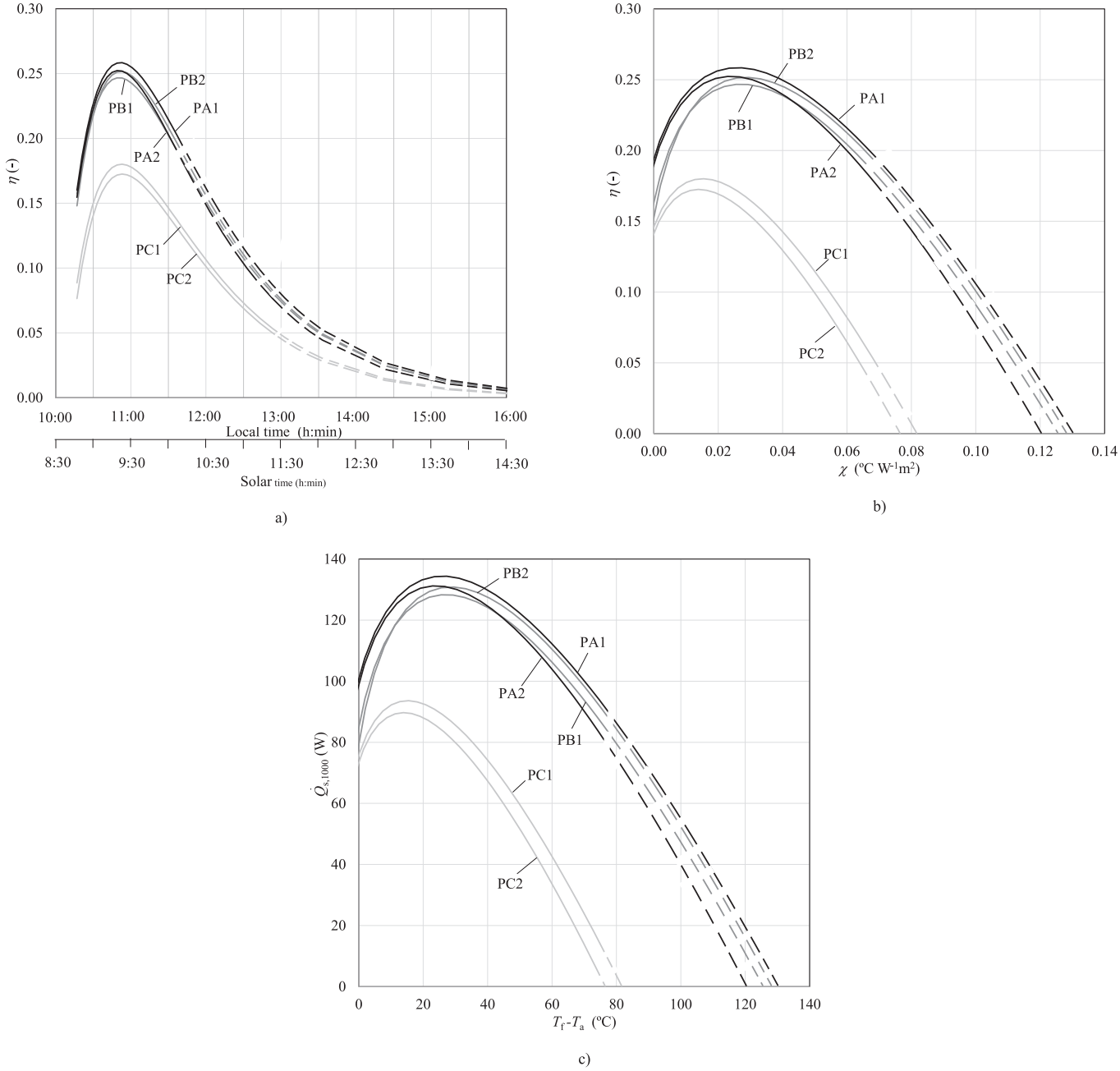

Fig. 5. Performance curves for each cooker: a) η vs time, b) η vs χ and c) $\dot{Q}_{s,1000}$ vs $T_f - T_a$.

Table 2
Particular points of the efficiency curve.

Cooker	χ_V (°Cm^{2}W^{-1})	η_V (–)	χ_C (°Cm^{2}W^{-1})	η_C (–)	χ_H (°Cm^{2}W^{-1})	η_H (–)
PA1	−0.006	0.128	0.026	0.258	0.130	0.000
PA2	0.006	0.121	0.024	0.252	0.120	0.000
PB1	−0.003	0.128	0.027	0.247	0.126	0.000
PB2	−0.002	0.115	0.029	0.252	0.128	0.000
PC1	−0.006	0.059	0.015	0.180	0.082	0.000
PC2	−0.007	0.046	0.014	0.172	0.077	0.000

degradation of the mirrors. Specifically, their optical efficiency is lower than that of the other four tested cookers. In Fig. 5, the curves for cookers PC1 and PC2 are not exactly parallel to those of cookers PA1, PA2, PB1, and PB2, but some parallel behaviour is evident. By observing the separation between these two sets of curves, the difference in optical efficiency between the four cookers with good mirrors and the two with degraded mirrors is estimated to be around 10%.

The differences between the χ_H values of the four cookers with the

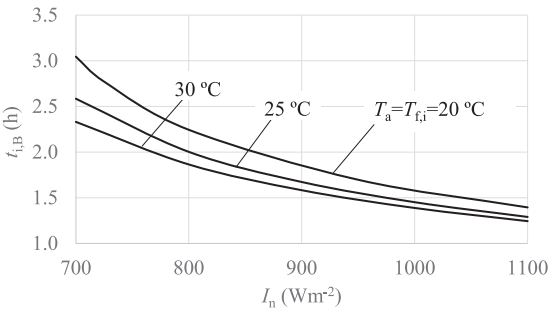

Fig. 6. Time taken to heat 2 kg of water from initial temperature, equal to ambient air temperature, to boiling temperature at sea level, using cooker PA1.

best performances are also small. The average value of χ_H for these four cookers is 59% greater than the average value of χ_H for the other two cookers.

When cooking soup at an atmospheric pressure close to 1 atm, the water boiling point is just 5 °C greater than the upper limit of the experimental load temperature range considered in the curve-fitting procedure used to derive the time load temperature evolutions expressed by Eq. (5). Thus, the error in extrapolating the derived fitting function to estimate the efficiency, when the load temperature is between 95 and 100 °C, is thought to be negligible. For clear sky conditions, with a solar irradiance (I_n) of 1000 Wm^{-2}, and an ambient temperature (T_a) of 20 °C, the specific temperature difference (χ), when the water starts boiling, at 100 °C, is equal to 0.08 °C m^2 W^{-1}. This means that, even under these good conditions, during a period when the sun elevation varies from 45° to near its maximum value at a latitude of 40°, the cookers PC1 and PC2 can not boil 2 kg of water. These two cookers could boil water at sea level only on very hot days, with ambient temperatures of around 40 °C, but the time taken to reach boiling point, even under those ideal conditions, is expected to be enormous.

In the present work, the period of time, $t_{i,B}$, needed to raise the temperature of the load from ambient temperature, $T_{f,a}$=T_a, to the boiling point of water at sea level, $T_{f,b} = T_{f,B} = 100\,^oC$, for solar irradiance I_n in the range 700 to 1100 Wm^{-2} and ambient temperature T_a equal to 5 °C, 20 °C and 35 °C, is equal to the value $t_{a,b}$ calculated analytically by Eq. (21). Fig. 6 shows the predicted time period $t_{i,B}$ required to heat 2 kg of water, using cooker PA1. The impact of the initial value of the load temperature on the time period $t_{i,B}$ is significant mainly when the solar irradiance is low. Under clear sky conditions at about 40° latitude, with solar irradiance close to 1000 Wm^{-2}, the time needed to start boiling water, when making 2 kg of soup, using a Pucca cooker with new glass mirrors positioned for high sun elevation, is estimated to be around 1.5 h when the average sun elevation during the cooking process is about 54°.

If $t_{i,B}$ was predicted by a function derived from Eq. (3), i.e., by following the approach based on the linear trend for the efficiency curve, the obtained values would be smaller than those considering the non-linear trend of the efficiency curve that is associated with function derived from Eq. (5). In case of PA1, the value would be $t_{i,B}$ 5% smaller when$I_n = 1000$ Wm^{-2} and$T_a = 20$ °C. It is also important to mention that the ASAE S580.1 procedure [16] stipulates that some data points from the initial portion of the cooker performance curve should not be used to derive the linear regression performance curve. Moreover, the time interval between recorded points using this protocol could be up to 10 min, which is much greater that the time interval of 10 s adopted in the present work. Thus, if the constants of Eq. (3) were determined using the ASAE S580.1 procedure, the value of $t_{i,B}$ would be greater than 5%. The difference between $t_{i,B}$ values obtained using linear and non-linear trends for the efficiency becomes more important for solar cooker designs where the distance between points V and C, shown in Fig. 1, is significant. Thus, even though the approach supported by the curve fitting expressed by Eq. (5) is more complex than the approach by the curve fitting expressed by Eq. (3), it was used here because it is more general, i.e., it is not limited to cases with a linear efficiency curve. Other research teams may wish to use this approach because it produces a better curve fit to the evolving temperature of the load in sensible heating tests.

The performance of a solar cooker with a funnel reflector design, previously investigated, is quite similar to that of the Pucca cooker. The tests in these earlier works [30,31] were conducted following the recommendation to perform tests around solar noon and assuming a linear trend for cooking power. This assumption implies that the load temperature closely follows the trend expressed by Eq. (3), and that the efficiency curve is linear. The deviation from this linear trend during the initial period of the curve was relatively small, as some of the initial measurement points were excluded from the linear cooking power regression. Additionally, this small deviation may be attributed to the fact that the difference between the minimum and maximum sun elevation values during those tests was significantly smaller compared to the conditions in the present study.

Alonso et al. [12] highlighted several issues that make the comparison of solar cookers challenging and presented a table with performance data for a wide range of solar cooker types, assuming a linear trend for the efficiency curve. One weakness of this approach is that the opto-thermal ratio values for cookers tested with water are questionable. It is suggested that tests be conducted with alternative fluids, such as glycerine, to improve reliability. The comparison task becomes even more difficult to conduct and present clearly as a complement to the present work, for several reasons. The primary reason is that the procedure adopted in this study is based on an efficiency curve with a non-linear trend, which has not yet been used to report the performance of many solar cooker designs.

Alonso et al. [12] tested their novel solar cooking system with two different receiver configurations. Configuration C1 used a thick glass washing machine window, while configuration C2 featured an enclosure made of a wooden box with cork insulation. The plots presented by Alonso et al. [12] show that the efficiency curve follows a linear trend with acceptable accuracy. Therefore, the two characteristic performance curves, which relate the time required for the load to reach a given temperature to the specific temperature difference, are also valid. In their study, Alonso et al. [12] calculated the specific temperature difference using direct normal solar irradiance rather than global normal solar irradiance. The actual normal intercept areas of the cooking system for configurations C1 and C2 are 0.546 m^2 and 0.476 m^2, respectively. These values are close to the area of the Pucca solar cooker, which is 0.52 m^2. The tests for the solar cooking systems with configurations C1 and C2 were performed with 1.9 kg of water, which is similar to the 2 kg used in the Pucca solar cooker tests.

A comparison is made using the performance curves from Fig. 13 of Alonso et al. [12] and Fig. 6, focusing on the time required for water to reach 100 °C during a summer day. The average ambient temperature is 30 °C, with global normal radiation of 1000 Wm^{-2}, direct normal radiation of 900 Wm^{-2}, and an initial water temperature of 30 °C. The estimated heating times are as follows: i) 95 min to heat 1.9 kg of water in configuration C1, ii) 78 min to heat 1.9 kg of water in configuration C2 and iii) 83 min to heat 2.0 kg of water in the Pucca Cooker PA1. From Eq. (1) it can be demonstrated that the average efficiency associated with the sensible heating test of a given fluid from initial value to the final value, for a given solar irradiance is proportional to the specific cooking rate Θ. The obtained values for the ratio Θ, in kg h^{-1} m^{-2}, are as

follows: 2.52 for configuration C1, 3.07 for configuration C2 and 2.78 for the Pucca Cooker PA1. The performance of the Pucca Cooker would likely improve even further with dual-axis solar tracking. While neither of the cooking systems is foldable, in the authors' opinion, the Pucca Cooker is a more robust system and requires less space compared to the novel cooking system with an advanced tracking system, as investigated by Alonso et al. [12] Based on user experience with the Pucca cooker, it can successfully cook most foods on sunny days within 2 to 3 h, requiring only a single tracking adjustment at the start of the cooking process. While an automatic tracking system could be developed, it is unnecessary, as is the case with most low to medium cooking speed solar cookers of the panel or box type.

In the study by Ruivo et al. [31], the influence of aperture area on the performance of a solar funnel cooker operating at high sun elevations was investigated using 1.736 kg of glycerine. The thermal capacitance of the glycerine load was approximately 5232 J °C^{-1}, which corresponds to 62.5% of the thermal capacitance used in tests with the Pucca solar cookers. The largest solar cooker tested by Ruivo et al. [31] had an aperture area of 0.5 m^2. Under the same summer conditions as mentioned above, the time required to heat the glycerine from 30 °C to 100 °C was 54 min. If 2 kg of water were used instead, a rough estimate for the specific cooking rate Θ would be 2.79 kg h^{-1}m^{-2}, which is almost equal to the value obtained for the Pucca solar cooker PA1. However, it is important to note that this estimate may contain some error, due to factors such as the differences in thermal properties between water and glycerine, as well as variations in sun elevation during the tests conducted by Ruivo et al. [31] and those with the Pucca solar cooker PA1. It is also important to note that the study by Ruivo et al. [31] relied on a linear trend for the efficiency curve derived from experimentally measured data, but it did not take into account the data from the initial part of the curve. The plots in Fig. 5 of Ruivo et al. [31] also show the existence of a point C, with a value of χ_C close to 0.02 °C m^2 W^{-2}. This suggests that the performance curves in their study could have been derived with greater accuracy by using the fitting method expressed in Eq. (5).

Considering test no. 29 reported in the study by Tomassetti et al. [19], the aperture area of the Kimono K2 prototype is close to that of the Pucca solar cooker. For this test, in which the initial and final water temperatures were 40 °C and 90 °C, respectively, the specific cooking rate Θ is estimated to be 2.22 kg h^{-1} m^{-2} for a water temperature increase of 50 °C. As mentioned earlier, the specific cooking rate for the Pucca solar cooker PA1 is estimated to be 2.78 kg h^{-1} m^{-2} for heating water from 30 °C to 100 °C, corresponding to a temperature increase of 70 °C. If Tomassetti et al. [19] had considered this larger temperature difference, the specific cooking rate for the Kimono K2 would be significantly lower than 2.22 kg h^{-1} m^{-2}. A rough estimate suggests that it might be on the order of 60% of the corresponding specific cooking rate for the Pucca solar cooker PA1.

Esen [13] conducted experiments using a more complex cooking system with an aperture area comparable to that of two Pucca solar cookers. Six sequential sensible heating tests were performed on a single day, each using 7 kg of water initially at 40 °C. The first five tests successfully reached a final temperature of 97 °C. The adopted load ratio was 7.3 kg m^{-2}, which is relatively high and close to the value recommended by the Standard ASAE S580.1 [16].

The third test was the shortest, lasting only 60 min (from 12:30 to 13:30), whereas the first and fifth tests lasted approximately 2.5 h and 2 h, respectively. Examination of the plots reported in Esen [13] suggests that the longer duration of the first test can be attributed to two main factors. First, the aluminium plate was not preheated, and its initial temperature was lower than that of the water. Second, the solar irradiance during this test was lower than the levels observed between 11:00 and 15:00 solar time.

For the first test, the average cooking power per unit aperture area is estimated to be about 470 W m^{-2}. Given that the average solar irradiance during this test was close to 1000 W m^{-2} [13], the corresponding average efficiency is approximately 0.47. However, considering the variation in solar irradiance from 350 to 850 W m^{-2} [13], the efficiency for this test is more conservatively estimated at around 0.32.

Analysis of the water temperature evolution (Fig. 3 in Esen [13]) shows that, in the first test, the rate of temperature increase rises gradually with time, except during the initial 30 min, when the plate temperature was lower than that of the pot and water. In the third test, the temperature rise rate remains nearly constant, while in the remaining tests it decreases with time. For the two sequential tests performed with edible oil, the rate of temperature increase generally rises with time, again with the exception of the initial 30 min of the first test [13].

Cooking experiments with different food items were repeated for each of the three heat-transfer fluids investigated by Esen [13]. In the case of cooking 0.5 kg of potatoes in 0.4 kg of water, the average cooking time over three tests was 63 min. The total mass of the load was therefore 0.9 kg, corresponding to a specific cooking rate of 0.89 kg h^{-1} m^{-2}. This value is significantly lower than the previously reported value of 2.78 kg h^{-1} m^{-2} for the Pucca Cooker PA1.

In a real cooking experiment conducted with the Pucca solar cooker, 2 kg of food were used to prepare a vegetable soup (see Appendix A). The total cooking time was approximately 2 h, corresponding to a specific cooking rate of 1.92 kg h^{-1} m^{-2}, which is more than double that reported by Esen [13]. The initial temperature of the ingredients and water was approximately 26 °C. The cooking process began at about 10:10 local time, reached boiling at around 12:00, and finished at approximately 12:10, i.e., about one hour before solar noon. If the cooking process had started one hour closer to solar noon, the specific cooking rate would be expected to be higher than 1.92 kg h^{-1} m^{-2}, mainly due to increased average solar irradiance during that period. For a more reliable comparison, it would be helpful if Esen [13] had reported the water temperature–time curve during the potato cooking experiment, as this would increase confidence in the conclusions drawn from comparing the two systems.

It is presumed that the potato cooking experiments by Esen [13] were performed close to solar noon and that the water temperature at the start of cooking was around 40 °C, as reported for sequential tests using water as the load. If this assumption is correct, then the reported specific cooking rate of 0.89 kg h^{-1} m^{-2} would be even lower if the cooking process had instead started with water and potatoes at 26 °C. Since the exact initial conditions are not clearly specified, this comparison nevertheless suggests that the Pucca solar cooker is a promising solar cooking device.

For example, if two Pucca solar cookers were used to cook 2 kg of ingredients for soup starting around 11:30 solar time, the cooking duration could reasonably be expected to decrease from 2 h to approximately 1 h. If the same two cookers were used to cook only 0.9 kg of food, the same load used in the potato cooking experiments by Esen [13], and the process started at around 11:30 solar time, the cooking time could be expected to fall within the range of 30 – 40 min. These estimates apply to clear summer conditions.

Under clear-sky winter conditions, the specific cooking rate of the Pucca solar cooker is expected to be lower and may become comparable to that of the system tested by Esen [13], particularly if the cooking process begins after a two- to three-hour preheating period. This assessment is based on the reported test results for both systems as well

Table 3
Time required to heat 2 kg of water from 20 °C to 100 °C using cookers PB1 and PB2, with an ambient temperature of 20 °C and a global solar irradiance of 1000 W m^{-2}.

Cooker	PB1	PB2
Date of experiment	16 July 2024	
Time $t_{i,B}$ (s)	6725	6454
Date of experiment	17 July 2024	
Time (s)	6143	6079
Date of experiment	19 July 2024	
Time $t_{i,B}$ (s)	6227	6257
Average time value (s)	6365	6263
Date of experiment	27 May 2022	
Time $t_{i,B}$ (s)	6053	5912

as the author's practical experience as a user of solar cookers.

Because the exact starting time of the cooking process in Esen's study is unknown, and because it is unclear whether the cooking chamber and pot were preheated, a rigorous and quantitative comparison between the results reported by Esen [13] and those obtained with the Pucca solar cooker is not possible. Assuming that the cooking pot initially had the same temperature as the food items, the specific cooking rate would likely increase if a massive cooking pot were preheated. Under this assumption, the performance could surpass that reported for Pucca solar cooker PA1. To draw reliable and definitive conclusions, a side-by-side experimental comparison of both systems under identical conditions is recommended.

4.3. Performance data from the side by side tests of three solar cookers

As previously mentioned, a series of additional tests was conducted in July 2024 to investigate the reproducibility of the results from the single test performed in May 2022. This set of experiments involved testing three of the solar cookers side by side, at the same location where the tests were conducted in May 2022.

Using the data summarized in Appendix B, the times $t_{i,B}$ needed to raise the load temperature from the ambient temperature, $T_{f,a}=T_a$, to the boiling point of water at sea level, $T_{f,b} = T_{f,B} = 100°C$, under solar irradiance $I_n = 1000$ Wm^{-2} and an ambient temperature $T_a = 20$ °C were estimated. These values of $I_n = 1000$ Wm^{-2} and $T_a = 20$ °C are not measured values, but rather assumed constant values that closely approximate the average experimentally observed in the various tests. When using Eq. (22), I_n=1000 Wm^{-2} can be treated as a reference or normalized value of solar irradiance, which closely matches clear sky conditions during a relatively short tests, similar to the conditions under which the performance of photovoltaic panels is reported. Table 3 presents the values calculated from the test results of two cookers with high-quality glass mirrors, PB1 and PB2, on the 16th, 17th, and 19th of July 2024. The table also includes the average values from the tests conducted in July 2024, as well as the results from the single experiment carried out in May 2022.

Taking the average time value for each cooker tested in July 2024 (as shown in Table 3) as a reference, the following observations were made: i) the maximum relative deviation of 5.7% occurred for the time of cooker PB1, tested on 16th July 2024 and ii) the relative deviations for cookers PB1 and PB2 tested on 27 th May 2022, compared to the average values from the July 2024 tests, were 4.9% and 5.6%, respectively.

Although the manual tracking of the solar cookers was not perfect, the deviations in the time duration $t_{i,B}$ estimated for the different days with cookers PB1 and PB2 are relatively small. Therefore, the reproducibility of the results can be considered acceptable. The times $t_{i,B}$ estimated from the tests conducted in May 2022 are slightly shorter than the average values obtained in July 2024. This difference can likely be attributed to minor degradation of the mirrors and slight variations in the tracking accuracy of the cookers.

The average sun elevation during the experiments in May 2022 and July 2024 with cookers PB1 and PB2 were 53.5° and 51.6°, respectively. The difference in the average solar angle between May 2022 and July 2024 accounts for the minor differences observed in the results. As mentioned in Section 3.1, it is expected that the cookers positioned for high sun elevation achieve optimal optical performance when the solar altitude angle is close to 53°. In the May 2022 experiment, the average solar angle was closer to this expected optimum.

5. Conclusions

Six robust funnel-shaped solar cookers were tested simultaneously, on a single test, on the roof terrace of a family house on 27th May 2022. The following cookers were made of concrete, and glass mirrors showing different levels of mirror surface deterioration: two new cookers with brand new glass mirrors, two used cookers with mirrors in good condition, and two cookers with mirrors in bad condition. Identical cooking vessels containing identical amounts of water were used. The cookers were tilted for high sun elevation and tested before solar noon. The variation in the sun elevation during the single experiment was not negligible. A second-degree polynomial with an exponential argument was used to fit the temperature of the load as a function of time for each cooker, enabling the prediction of the non-linear trend for the efficiency as function of the specific temperature difference.

The results showed that the performances of those cookers with mirrors in bad condition were poor. They had difficulty in boiling 2 kg of water. The cookers with old mirrors in good condition, i.e., those that had been used for several years, produced results almost as good as the new cookers with new mirrors. The influence of the initial water temperature and solar irradiance on the time needed to boil water was estimated by using a more accurate function than those usually employed in procedures based on a linear efficiency curve.

A minor reduction in the performance of the cookers was observed from May 2022 to July 2024. However, these small differences support the reliability and usefulness of the adopted enhanced evaluation protocol, especially when the efficiency or cooking power curves deviate from the typically expected linear trend. The commonly used procedures—based on linear regression of the cooking power or efficiency curves to report standardized cooking power, the opto-thermal ratio of a cooker, and the water boiling time derived from the first figure of merit (obtained from a stagnation test without load), as well as the second figure of merit (from a test with load)—may be questionable for certain cooker designs. Therefore, testing multiple solar cookers side by side, as in the present study, is crucial for accurately assessing performance differences.

The first Pucca solar cooker was built around 15 years ago using brand-new glass mirrors, which have remarkably maintained their reflectivity with little to no noticeable deterioration over time. In contrast, some models made with recycled glass mirrors, intended to reduce production costs and enhance sustainability, have shown signs of wear and reduced effectiveness.

As a panel-type solar cooker, the Pucca is capable of preparing meals for up to four people in about two hours. One of its major advantages is that it does not require constant repositioning to track the sun, allowing users to focus on other tasks, such as academic research, teaching, errands, resting, housework, or agricultural work. Although the cooker is not intended for conventional frying, it excels at baking items like bread

and cakes. During colder months, when heat loss is more significant, cooking smaller portions is recommended.

The approach adopted in this study, based on a non-linear efficiency curve, provides a more comprehensive assessment than analyses relying solely on linear efficiency or power performance curves. Nevertheless, despite its advantages over more commonly used methods, the proposed approach is not intended to be applicable under the following conditions: (i) when the mass of evaporated water is non-negligible; (ii) during relatively long cooking periods in which solar irradiance varies significantly, such as shortly after sunrise or before sunset; and (iii) when the rate of water temperature increase during the sensible heating period is enhanced by the use of thermal energy storage systems, including phase-change materials or large sensible heat storage media.

CRediT authorship contribution statement

Celestino Rodrigues Ruivo: Writing – review & editing, Writing – original draft, Supervision, Methodology, Formal analysis. **Semaan Azize:** Investigation. **Xabier Apaolaza-Pagoaga:** Writing – review & editing, Investigation. **Antonio Carrillo-Andrés:** Writing – review & editing.

Declaration of competing interest

The authors declare that they have no known competing financial interests or personal relationships that could have appeared to influence the work reported in this paper.

Acknowledgements

The authors would like to acknowledge Mr. Dave Oxford, of SLiCK-solarstove UK, for his valuable help in reviewing and revising the manuscript for grammar and syntax.

Semaan Azize, student of Master in Thermal Energy Mechanical Engineering of Polytech Nantes in France participated in this research during his traineeship as Erasmus student at University of Algarve from 20th May 2024 to 19th August 2024.

This research was funded in part by the Fundação para a Ciência e a Tecnologia, I.P. (FCT, https://ror.org/00snfqn5816) under Grant (https://doi.org/10.54499/UIDB/50022/2020, https://doi.org/10.54499/UIDP/50022/2020, https://doi.org/10.54499/LA/P/0079/2020).

Appendix A. – Brief details on the construction, costs estimation, and practical use of the Pucca solar cooker

The Pucca solar cooker is capable of cooking food even under strong windy conditions. Moreover, its robust design allows it to remain permanently outdoors, as it can withstand strong winds and rain, features that are often limitations in most conventional solar cooker designs. To avoid prohibitive transportation costs, this cooker should be manufactured locally. Based on the authors' experience and knowledge, the estimated cost of constructing the required moulds is approximately €150 in India and €400 in Portugal. As the cooker has not yet been commercialized, the authors can only provide an estimated unit cost for mass production, which is expected to be around €150 in India and €250 in Portugal. However, in the absence of actual commercialization, further discussion of market pricing is beyond the scope of this paper.

The Pucca cooker design is affordable for use year-round on sunny days and in a variety of climates worldwide. Based on the extensive experience of the user, the Pucca cooker can also be easily operated under low sun elevation on a sunny summer day, typically during three hours period after sunrise or three hours before sunset or throughout a sunny winter day. For optimal cooking on a cold, sunny day, the mass of food should be smaller than on a hot, sunny day. The actual design does not achieve optimum optical efficiency at certain latitudes, particularly when the sun is near the zenith (about two to three hours around solar noon). However, a minor modification to the middle piece could improve performance during this period. Fig. A1 shows the set of moulds used for constructing the three main concrete pieces. Fig. A2 shows, as an example, two litres of vegetable soup prepared in a Pucca solar cooker on the 28th July, 2024.

Fig. A1. Moulds and concrete pieces of the Pucca solar cooker.

a)

c)

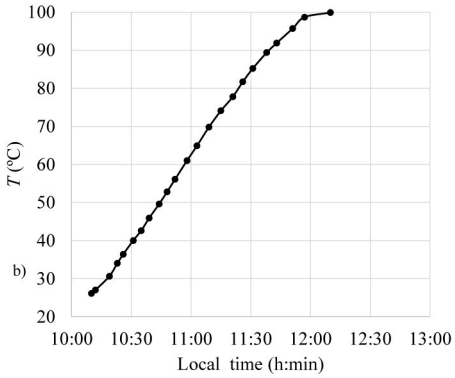

b)

d)

Fig. A2. Vegetable soup cooked in the Pucca solar cooker on 28 July 2024: a) pot with ingredients before cooking; b) pot with ingredients after cooking; c) final prepared soup; and d) time evolution of the ingredient temperature during cooking.

Appendix B. – Complementary set of tests to check the reproducibility of the performance results

The performance results presented in Section 4 are based on data from a single experiment conducted on 27th May 2022, during which six Pucca solar cookers were tested concurrently. The data in this appendix show the results of experiments conducted in July 2024, when the average solar elevation values were similar to those during the May 2022 tests.

This complementary set of tests was performed at the same location but used only the available cookers PB1, PB2, and PC1. Cooker PA1, equipped with new mirrors, was not used, as it was being utilized by a Portuguese family 500 km from Faro. Similarly, Cooker PA2, also with new mirrors, was unavailable because it was being used at the University of Malaga for a project unrelated to the scope of the present study. Cooker PC2 was not used either, as its degraded glass mirrors had been replaced with high-reflectivity mirrors, and it is currently being used at the University of Malaga for a separate research project beyond the scope of this work.

Tables B1 and B2 present the data from the tests conducted in July 2024, starting at 10:10 am, as in the May 2022 experiment. The same cooking vessels and the same amount of water were used in both sets of tests.

Table B1
Data from additional tests conducted in July 2024 with cookers PB1 and PB2.

Date	16 Jul 2024		17 Jul 2024		19 Jul 2024	
Cooker	PB1	PB2	PB1	PB2	PB1	PB2
Initial sunelevation (°)	42.8	42.7	42.6	42.6	42.4	42.4
Final sun elevation (°)	61.2	61.1	60.5	60.3	60.3	60.7
Average air velocity (m s^{-1})	1.2	1.2	1.0	1.0	not measured	
Average air temperature (°C)	26.7	26.7	29.1	29.0	32.5	32.5
Average solar irradiance (Wm^{-2})	988.7	988.5	974.6	974.5	930.0	930.5
$c_{2,0}$(°C)	166.6	199.4	171.3	192.7	181.9	204.8
$c_{2,1}$(°C)	-242.6	-300.0	-260.6	-293.0	-261.5	-296.8
$c_{2,2}$(°C)	102.8	126.1	115.0	126.4	108.8	120.5
t_2(s)	5347	6637	5201	6042	6031	7178
RMSD(°C)	0.157	0.197	0.192	0.218	0.111	0.122

Table B2
Data from additional tests conducted in July 2024 with cooker PC1.

Date	16 Jul 2024	17 Jul 2024	19 Jul 2024
Initial sunelevation (°)	42.7	42.6	42.4
Final sunelevation (°)	71.8	71.5	70.1
Average air velocity (m s^{-1})	1.3	1.0	not measured
Average air temperature (°C)	27.0	29.8	33.2
Average solar irradiance (Wm^{-2})	987.2	978.4	938.1
$c_{2,0}$(°C)	112.3	109.4	122.7
$c_{2,1}$(°C)	-155.1	-155.7	-162.9
$c_{2,2}$(°C)	69.1	72.7	68.8
t_2(s)	4729	4387	5638
RMSD(°C)	0.318	0.364	0.400

Data availability

Data will be made available on request.

References

[1] https://www.vatsalya.org/environment. Accessed on 11th August 2024.
[2] https://solarcooking.fandom.com/wiki/Brahma_Kumaris. Accessed on 11th August 2024.
[3] https://lytefire.com/en. Accessed on 11th August 2024.
[4] https://partnerswithsun.com/. Accessed on 11th August 2024.
[5] https://solarcooking.fandom.com/wiki/Delicias_del_Sol. Accessed on 11th August 2024.
[6] https://solarcooking.fandom.com/wiki/Le_Pr%C3%A9sage. Accessed on 11th August 2024.
[7] E.A. Padonou, G.C. Akabassi, B.A. Akakpo, B. Sinsin, Importance of solar cookers in women's daily lives: a review, Energy Sustain. Dev. 70 (2022) 466–474, https://doi.org/10.1016/j.esd.2022.08.015.
[8] P.K. Kajumba, D. Okello, K. Nyeinga, O.J. Nydal, Assessment of the energy needs for cooking local food in Uganda: a strategy for sizing thermal energy storage with cooker system, Energy Sustain. Dev. 67 (2022) 67–80, https://doi.org/10.1016/j.esd.2022.01.005.
[9] A. Kumar, A. Karn, C. McGregor, V.P. Singh, A critical analysis of paradigm shifts from domestic solar cooking to institutional solar cooking technologies, Renew. Sustain. Energy Reviews. 218 (2025) 115840, https://doi.org/10.1016/j.rser.2025.115840.
[10] S. Verma, S. Banerjee, R. Das, A fully analytical model of a box solar cooker with sensible thermal storage, Sol. Energy 233 (2022) 531–542, https://doi.org/10.1016/j.solener.2021.12.035.
[11] R.K. Goyal, M. Eswaramoorthy, Theoretical and experimental analysis of box-type solar cooker with sensible heat storage, Sol. Energy 268 (2024) 112273, https://doi.org/10.1016/j.solener.2023.112273.
[12] I. Alonso, P.A. Bibiloni-Mulet, J. Vidal-Noguera, Y. Torres, A. Moià-Pol, V. Canals, V. Martínez-Moll, Thermal performance assessment of a novel concentrating solar cooker with equatorial tracking from full load tests, Sol. Energy 300 (2025) 113812, https://doi.org/10.1016/j.solener.2025.113812.
[13] M. Esen, Thermal performance of a solar cooker integrated vacuum-tube collector with heat pipes containing different refrigerants, Sol. Energy 76 (2004) 751–757, https://doi.org/10.1016/j.solener.2003.12.009.
[14] S.C. Mullick, T.C. Kandpal, A.K. Saxena, Thermal test procedure for box-type solar cookers, Sol. Energy 39 (1987) 353–360, https://doi.org/10.1016/S0038-092X(87)80021-X.
[15] S.C. Mullick, T.C. Kandpal, Thermal test procedure for a paraboloid concentrator solar cooker, Sol. Energy 46 (1991) 139–144, https://doi.org/10.1016/0038-092X(91)90087-D.
[16] ASAE S580.1 NOV2013, Testing and reporting solar cooker performance, American Society of Agricultural Engineers, Michigan, USA, 2013.
[17] M. Collares-Pereira, A. Cavaco, A. Tavares, Figures of merit and their relevance in the context of a standard testing and performance comparison methods for solar box – cookers, Sol. Energy 166 (2018) 21–27, https://doi.org/10.1016/j.solener.2018.03.040.
[18] S.M. Ebersviller, J.J. Jetter, Evaluation of performance of household solar cookers, Sol. Energy 208 (2020) 166–172, https://doi.org/10.1016/j.solener.2020.07.056.
[19] S. Tomassetti, A. Aquilanti, P.F. Muciaccia, M. Muccioli, G. Di Nicola, Experimental characterization of a panel solar cooker with adjustable geometry for sun tracking, Sol. Energy 287 (2025) 113178, https://doi.org/10.1016/j.solener.2024.113178.
[20] C.R. Ruivo, G. Coccia, G. Di Nicola, A. Carrillo-Andrés, X. Apaolaza-Pagoaga, Standardised power of solar cookers with a linear performance curve following the Hottel-Whillier-Bliss formulation, Renew. Energy 200 (2022) 1202–1210, https://doi.org/10.1016/j.renene.2022.10.041.
[21] C.R. Ruivo, Some features and research perspectives on standalone solar cooking devices, Reference Module in Materials Science and Materials Engineering, Elsevier, 2025, ISBN 9780128035818, https://doi.org/10.1016/B978-0-443-29210-1.00060-1.
[22] C. Ruivo, X. Apaolaza-Pagoaga, G. Coccia, A. Carrillo-Andrés, Proposal of a non-linear curve for reporting the performance of solar cookers, Renew. Energy 191 (2022) 110–121, https://doi.org/10.1016/j.renene.2022.04.026.

[23] G. Coccia, G. Di Nicola, M. Pierantozzi, S. Tomassetti, A. Aquilanti, Design, manufacturing, and test of a high concentration ratio solar box cooker withmultiple reflectors, Sol. Energy 155 (2017) 781–792, https://doi.org/10.1016/j.solener.2017.07.020.
[24] C. Ruivo, X. Apaolaza-Pagoaga, G. Di Nicola, A. Carrillo-Andrés, On the use of experimental measured data to derive the linear regression usually adopted for determining the performance parameters of a solar cooker, Renew. Energy 181 (2022) 105–115, https://doi.org/10.1016/j.renene.2021.09.047.
[25] J.A. Duffie, W.A. Beckman, Solar Engineering of Thermal Processes, fourth ed., Willey, 2013.
[26] P.J. Lahkar, R.K. Bhamu, S.K. Samdarshi, Enabling inter-cooker thermal performance comparison based on cooker opto-thermal ratio (COR), Appl. Energy 99 (2012) 491–495, https://doi.org/10.1016/j.apenergy.2012.05.034.
[27] A.A. Sagade, S.K. Samdarshi, P.S. Panja, Enabling rating of intermediate temperature solar cookers using different working fluids as test loads and its validation through a design change, Sol. Energy 171 (2018) 354–365, https://doi.org/10.1016/j.solener.2018.06.088.
[28] A.A. Sagade, X. Apaolaza-Pagoaga, C. Rodrigues Ruivo, A. Carrillo-Andrés, Concentrating solar cookers in urban areas: establishing usefulness through realistic intermediate temperature rating and grading, Sol. Energy 241 (2022) 157–166, https://doi.org/10.1016/j.solener.2022.06.007.
[29] C. Ruivo, A. Carrillo-Andrés, X. Apaolaza-Pagoaga, Experimental determination of the standardised power of a solar funnel cooker for low sun elevations, Renew. Energy 170 (2021) 364–374, https://doi.org/10.1016/j.renene.2021.01.146.
[30] X. Apaolaza-Pagoaga, A. Carrillo-Andrés, C. Ruivo, New approach for analysing the effect of minor and major solar cooker design changes: Influence of height trivet on the power of a funnel cooker, Renew. Energy 179 (2021) 2071–2085, https://doi.org/10.1016/j.renene.2021.08.025.
[31] C.R. Ruivo, X. Apaolaza-Pagoaga, A. Carrillo-Andrés, G. Coccia, Influence of the aperture area on the performance of a solar funnel cooker operating at high sun elevations using glycerine as load, Sustain. Energy Tech. Assess. 53 (2022) 102600, https://doi.org/10.1016/j.seta.2022.102600.